Zebrafish models for human FKRP muscular dystrophies

Genri Kawahara[1,2,5], Jeffrey R. Guyon[1,2,5], Yukio Nakamura[1,3] and Louis M. Kunkel[1,2,4,5,]*

[1]Division of Genetics, Program in Genetics, [2]Department of Genetics, [3]Department of Orthopaedics Surgery, Harvard Medical School, [4]Howard Hughes Medical Institute and [5]The Manton Center for Orphan Disease Research, Children's Hospital, Boston, MA, USA

Various muscular dystrophies are associated with the defective glycosylation of α-dystroglycan and are known to result from mutations in genes encoding glycosyltransferases. Fukutin-related protein (FKRP) was identified as a homolog of fukutin, the defective protein in Fukuyama-type congenital muscular dystrophy (FCMD), that is thought to function as a glycosyltransferase. Mutations in FKRP have been linked to a variety of phenotypes including Walker–Warburg syndrome (WWS), limb girdle muscular dystrophy (LGMD) 2I and congenital muscular dystrophy 1C (MDC1C). Zebrafish are a useful animal model to reveal the mechanism of these diseases caused by mutations in FKRP gene. Downregulating FKRP expression in zebrafish by two different morpholinos resulted in embryos which had developmental defects similar to those observed in human muscular dystrophies associated with mutations in FKRP. The FKRP morphants showed phenotypes involving alterations in somitic structure and muscle fiber organization, as well as defects in developing eye morphology. Additionally, they were found to have a reduction in α-dystroglycan glycosylation and a shortened myofiber length. Moreover, co-injection of fish or human FKRP mRNA along with the morpholino restored normal development, α-dystroglycan glycosylation and laminin binding activity of α-dystroglycan in the morphants. Co-injection of the human FKRP mRNA containing causative mutations found in human patients of WWS, MDC1C and LGMD2I could not restore their phenotypes significantly. Interestingly, these morphant fish having human FKRP mutations showed a wide phenotypic range similar to that seen in humans.

INTRODUCTION

Several muscular dystrophies have been associated with glycosylation defects of dystroglycan. Dystroglycan is a central component of the dystrophin–glycoprotein complex (DGC), a large protein complex essential for maintaining the integrity of the sarcolemma by connecting components of the extracellular matrix (ECM) to the internal cytoskeleton of the muscle fiber. No human diseases have been associated with the dystroglycan gene mutations. However, dag1-null mice showed embryonic lethality (1), suggesting that dystroglycan function is critical for normal embryogenesis. Mature dystroglycan consists of two isoforms (α- and β- dystroglycan) generated by post-translational cleavage of a precursor protein (2). Additionally, α-dystroglycan subunit is capable of binding to a

variety of laminin isoforms and the proteoglycan molecules agrin, perlecan and neurexins (2–5).

Several forms of muscular dystrophy are associated with the defective glycosylation of α-dystroglycan and are caused by mutations in six genes encoding putative glycosyltransferases: POMGnT1, POMT1, POMT2, Fukutin, fukutin-related protein (FKRP) and LARGE (6–13). These diseases include severe forms of congenital muscular dystrophy associated with structural brain defects and variable eye involvement such as Fukuyama-type congenital muscular dystrophy (FCMD), muscle–eye–brain (MEB) disease (14) and Walker–Warburg syndrome (WWS) (15). Mutations in the glycosyltransferase genes also cause much milder muscular dystrophies such as the limb girdle muscular dystrophies (LGMD) types 2I and 2K (16). In some cases, a spectrum of

*To whom correspondence should be addressed at: Program in Genomics, Children's Hospital Boston, Enders Rm 570, 300 Longwood Ave, Boston, MA 02115, USA. Tel: +1 6173556729; Email: kunkel@enders.tch.harvard.edu

disease severity can result from different mutations in any one of these putative glycosyltransferase genes (6,7). The pathology of these disorders has been attributed to the failure of the resulting hypoglycosylated dystroglycan to bind to components of the ECM (17).

FKRP was identified as a homolog of fukutin, the defective protein on FCMD (13,18). The primary protein sequence predicted from the gene sequence indicates homology to a class of proteins that are thought to function as glycosyltransferases, specifically mediating O-linked glycosylation. The role of FKRP in the glycosylation of α-dystroglycan remains unclear. FKRP has been proposed as a putative glycosyltransferase based on similar sequences to other glycosyltransferases; however, this activity has not been confirmed (19). Mutations in FKRP have been linked to variable phenotypes including congenital muscular dystrophy, also referred to as MDC1C, and LGMD2I that may or may not be accompanied by dilated cardiomyopathy. The range of phenotypic severity due to FKRP mutations is very large and is not usually observed for other genes involved with muscular dystrophy (18). Some reports of FKRP mutations include descriptions of founder mutations in the European population (826C > A, L276I) and the Tunisian population (1364C > A, A455D) (18,20,21). Moreover, recent reports showed that some mutations in FKRP gene caused WWS (953G > A, C318Y) and MEB (919T > A, Y307N) (22,23).

Zebrafish represent a good model to investigate genes involved in muscle development and degeneration, and they serve as a good model for muscular dystrophy (19,24–31). The zebrafish expresses orthologues of many DGC components (32). Zebrafish have glycosyltransferases with strong homology to the human forms including FKRP (33). Using a morpholino against FKRP, the resulting knocked down morphants showed an abnormal formation of muscle and eye analogous to the human diseases (34). These results demonstrate the possibility of the animal model of dysfunction of this glycosyltransferase.

In the present study, we have knocked down FKRP expression in the zebrafish using two different morpholinos and obtained the same phenotypes in the resulting morphants as previously reported (34). FKRP morphant embryos show defects in muscle organization, eye development and reduction in α-dystroglycan glycosylation. In addition, co-injection of a control FKRP mRNA or mutated FKRP mRNAs either corrected pathology or mimicked human clinical conditions. Interestingly, the developmental symptoms in the FKRP morphant were restored by injection of control FKRP mRNA, not by mutated human FKRP mRNAs. Moreover, injection of human FKRP restored the reduction of α-dystroglycan glycosylation and laminin binding to α-dystroglycan. Our data suggest that the fish model of human FKRP mutations is useful to investigate the pathogenesis associated with the FKRP gene and serves to elucidate the role of FKRP in developmental processes associated with the glycosylation of α-dystroglycan.

RESULTS

FKRP morphant morphology

We began the study of the function of FKRP in zebrafish embryo development by using two anti-sense morpholino oligonucleotides (MO) to disrupt the translation of FKRP mRNA during development. MO1 and MO2 were targeted to regions containing the 5'-untranslated region (MO2) and the start codon of fish FKRP mRNA (MO1). The binding regions of MO1 and MO2 were not overlapping. At 1 dpf, FKRP morphant injected FKRP MO1 (6 ng) and FKRP morphant injected FKRP MO2 (6 ng) had abnormal formation of their heads and eyes (Supplementary Data S1). Moreover, the organization of their muscles was abnormal in both FKRP morphants compared with controls. FKRP morphants displayed alterations in somite morphology observed as curved somite boundaries that are distinct from the regular v-shaped pattern observed in control MO injected embryos (Supplementary Data S1). At 1 dpf, mildly affected morphant embryos were also found to have curved tails and a slight curvature of the somite boundaries like previously reported (34). At 1 dpf, the frequency of observed abnormalities was correlated with injection of increasing amounts of both FKRP MO1 and 2 (Supplementary Data S2).

At 4 dpf, the frequency of observed developmental abnormalities was also found to correlate in a dose-dependant fashion with amounts of both FKRP MO1 and 2 injected (Supplementary Data S2). Injection of 6 ng of MO1 resulted in a mixture of different fish phenotypes with ∼40% of injected fish exhibiting developmental abnormalities, 40% appearing normal and 20% of them dead. Fish injected with 3 ng of MO2 also had a mixture of different phenotypes with 40% of injected fish exhibiting developmental abnormalities, 20% appearing normal and 40% of them dead. Injection of control morpholinos to both of MO1 and MO2 (mis-matched at 5 bases; see Materials and Methods) resulted in few observed abnormalities which were likely caused by the injection procedure (Supplementary Data S2).

FKRP morphant embryos lacked locomotor activity and did not respond to touch with the normal escape response observed in control embryos. Overall, FKRP morphants appeared to have a smaller eye size compared with controls (arrows in Fig. 1G and I) and many had inflated precardia (arrowheads in Fig. 1G and I). FKRP morphant embryos were also found to have an irregular arrangement of muscle fibers compared with control embryos (arrows in Fig. 2G and I). To better visualize the structure and organization of muscle fibers of the morphants, FKRP morphant and control embryos at 4 dpf were analyzed by birefringence assays (Figs 1 and 2). FKRP morphant embryos were found to have markedly reduced normal patterns of birefringence compared with control (Figs 1H and 1J and 2H and I). To confirm the knock down of the expression of fish FKRP with morpholino injection, endogenous FKRP protein was analyzed with antibodies against fish FKRP. In control MO1 and MO2, the FKRP directed antibody recognized 60 kDa protein on western blots, a size predicted by the fish FKRP sequence. The analysis of morphant 1 and 2 extracts showed that the expression of FKRP protein in morphants was substantially decreased compared with those of control MO1- and MO2-injected fish (Fig. 2K). Western blot results show that the morpholinos used in these injections were effective in knocking down the expression of FKRP during zebrafish development.
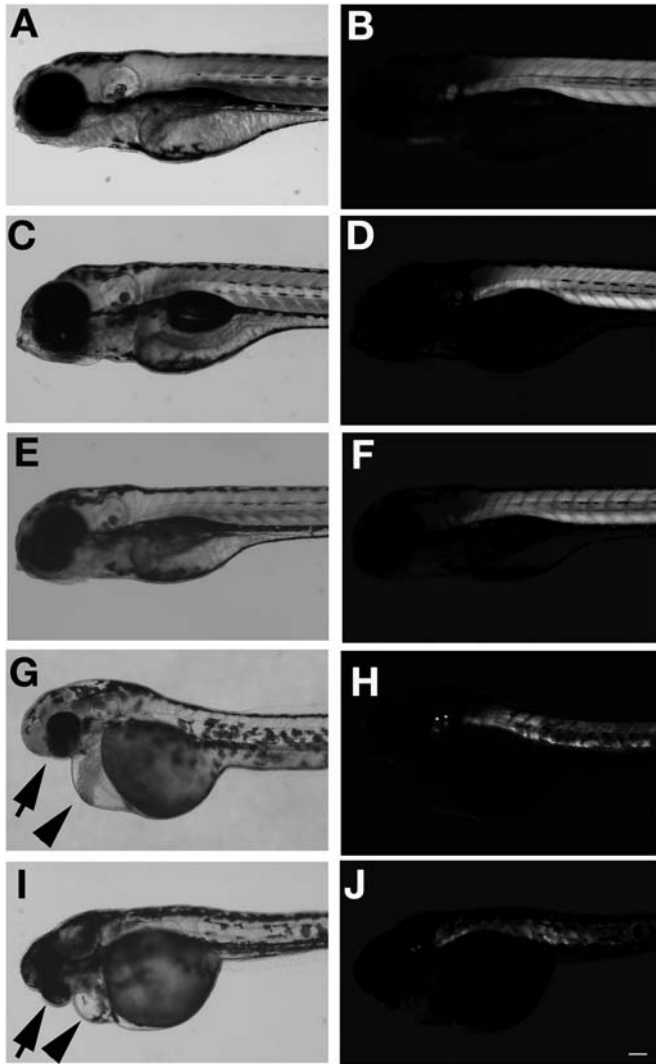
Figure 1. Head and body in FKRP morphant at 4 dpf. (**A** and **B**) wild-type fish. (**C** and **D**) Control MO1 injected fish. (**E** and **F**) Control MO2 injected fish. (**G** and **H**) FKRP MO1 injected fish. (**I** and **J**) FKRP MO2 injected fish. (A), (C), (E), (G) and (I) show bright images. (B), (D), (F), (H) and (J) show results of birefringence assay. Arrows show smaller eyes in affected fish. Arrowheads show inflated heart in affected fish. Bar: 100 μm.

Immunohistochemistry with muscle structure's components

To examine the expression of other muscle proteins, antibodies against dystrophin, β-dystroglycan, α-dystroglycan and myosin heavy chain (MHC, slow fiber) were used for immunohistochemistry on the morphant embryos. Dystrophin and β-dystroglycan expression at the myosepta appeared normal and identical to control (Fig. 3I and J); however, the immunostaining of these antibodies indicated that somite boundaries were misshapen with a curved appearance and a less distinct v-shaped structure as seen in controls with localized variation in reactivity to the antibodies along the lengths of the boundaries (Fig. 3I and J).

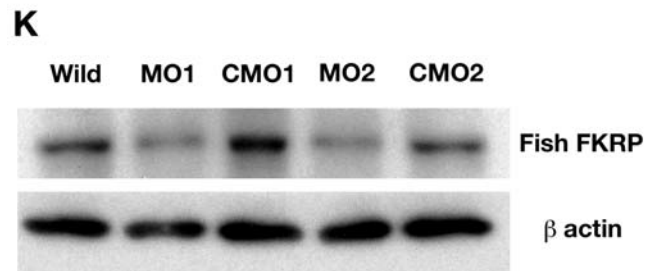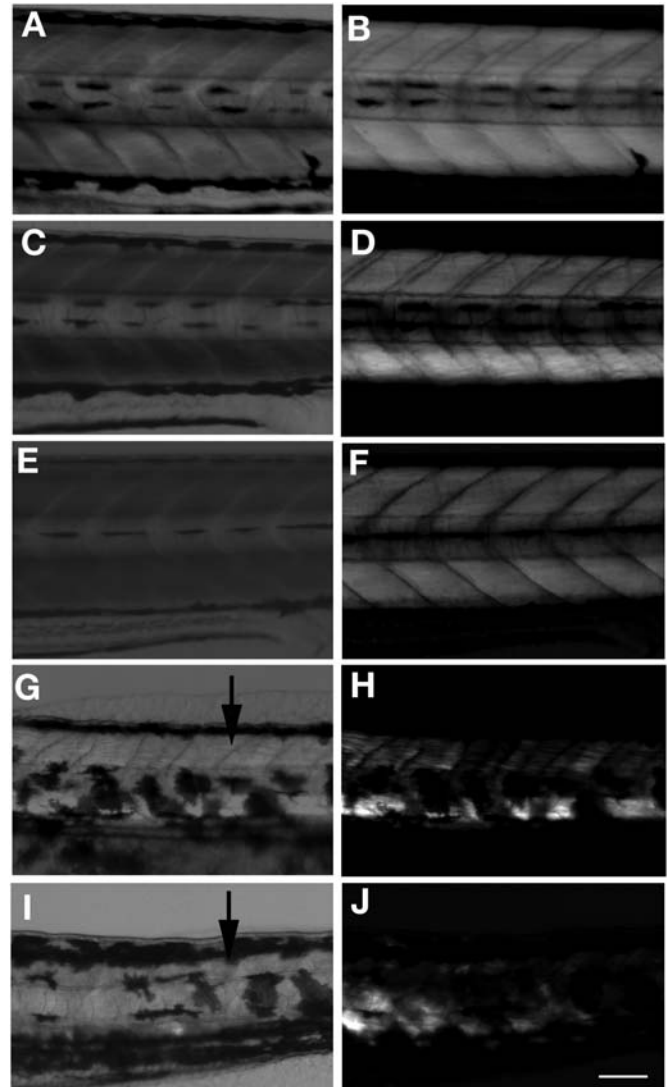To investigate the glycosylation of α-dystroglycan in FKRP morphant embryos, embryos at 4 dpf were immunostained

Figure 2. Body and muscle structures in FKRP morphant at 4 dpf. (**A** and **B**) Wild-type fish. (**C** and **D**) Control MO1 injected fish. (**E** and **F**) Control MO2 injected fish. (**G** and **H**) FKRP MO1 injected fish. (**I** and **J**) FKRP MO2 injected fish. (A), (C), (E), (G) and (I) show bright field pictures. (B), (D), (F), (H) and (J) show results of birefringence assay. Arrows highlight the disorganization of myosepta in FKRP morphants. Bar: 100 μm. (**K**) Immunoblot of protein extracts of 4 dpf wild-type fish and 4 dpf fish injected with FKRP MO1, MO2, control MO (CMO) 1 and 2.

with the antibody VIA4-1, which reacts specifically to glycosylated isoforms of α-dystroglycan (35). At 4 days, VIA4-1 staining was mainly observed in normal embryos at the somite boundaries (Fig. 3C and G). VIA4-1 staining of
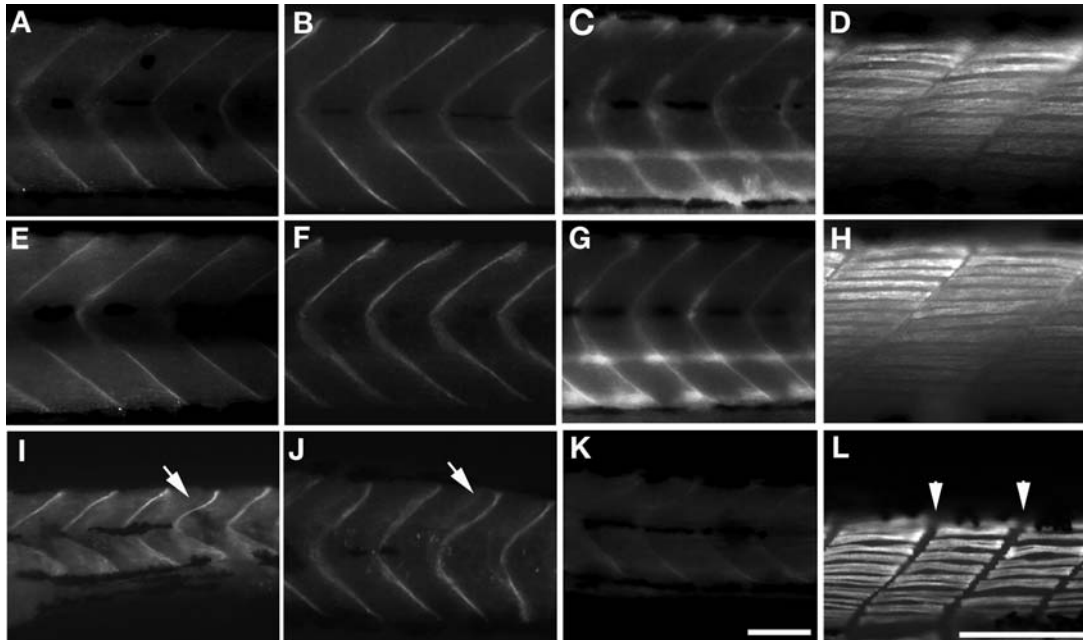
Figure 3. Immunostaining of FKRP morphant with antibodies against different muscle protein components. (**A**–**D**) wild-type. (**E** and **F**) Control MO2. (**I**–**L**) FKRP MO2. (A), (E) and (I) show the results of immunostaining with anti-dystrophin. (B), (F) and (J) show the results with the anti β-dystroglycan antibody. (C), (G) and (K) show the results with anti α-dystroglycan. (D), (H) and (L) show with anti-MHC. Arrows indicate the disturbance of myosepta in the FKRP morphant. Arrowheads show the gaps between myofibers at myosepta. Bar: 100 μm.

viable FKRP morphants showed a decreased reactivity to VIA4-1 (Fig. 3K) compared with controls.

Staining with anti-MHC demonstrated that the length of the myofibers appeared significantly shorter than the control and the gap between myofibers appeared wider compared with control (Fig. 3L), direct measurements given below.

Co-injection of normal or mutant mRNAs recapitulates human phenotypes

Human and fish FKRP mRNAs were co-injected with the morpholinos to determine whether they could rescue the developmental phenotypes. FKRP mRNA (100 pg) and 3 ng of FKRP MO2 were co-injected into 1-cell- or 2-cell-stage eggs. Co-injection of fish or human FKRP mRNA with MO was effective in the reduction of the number of fish affected with the developmental phenotype at 1 dpf (Supplementary Data S2) and 4 dpf (Fig. 4A). The percentage of affected fish and those which died was reduced compared with MO-injected fish, which indicated a partial rescue of the developmental phenotype by these mRNAs. However, co-injection of human FKRP mRNA bearing mutations was not as effective in the recovery of these developmental phenotypes (Fig. 4A). The percentage of recovered affected fish was variable among L276I-, C318Y- and A455D-mutated human FKRP mRNA injected fish (Fig. 4A). L276I-mutated fish showed generally better developmental rescue of the phenotypes; however, C318Y- and A455D-mutated fish had a high percentage of abnormal embryos similar to morphants with morpholino alone (Fig. 4A). The expression of mutant FKRP proteins bearing a c-myc-tag encoded from the injected

FKRP mRNAs was confirmed by anti c-myc antibodies (Fig. 4B).

To examine the recovery of normal development in muscle structures and eyes found in FKRP morphants (Figs 1G and I and 2G and I), we measured the results of normal and abnormal development. For muscle somites, the average control distance between myosepta was 85.2 μm. In FKRP control MO, the distance was similar with an average of 82.8 μm. FKRP morphant embryos showed an average distance of 72.4 μm between myosepta. The distance between myosepta in FKRP morphant embryos was significant compared with control ($P < 0.001$) (Fig. 4C).

Moreover, the normal distance between myosepta could be restored to normal by co-injection of fish or human FKRP mRNA ($P < 0.001$) (Fig. 4C). However, co-injection with human FKRP mRNA containing human mutant alleles was not as effective in recovery of these myosepta distances.

In wild-type fish embryos, the average eye diameter was 324 μm and in FKRP control MO injected embryos a similar average diameter of 317 μm was observed. FKRP morphants showed an average diameter of 200 μm (Fig. 4D). These measurements indicated that the size of eyes was significantly different ($P < 0.01$). When normal human or fish FKRP mRNA was co-injected, the reduced diameter of eye was returned to near control diameter (co-injection of human FKRP: 286 μm, fish FKRP: 295 μm). However, with co-injection of human FKRP mRNA with mutant alleles, this recovery to normal diameter was not observed. Moreover, measurements showed that phenotypes (eye diameter and the length between myosepta) of fish co-injected the mutated FKRP mRNA were different between the L276I, C318Y and A455D human FKRP
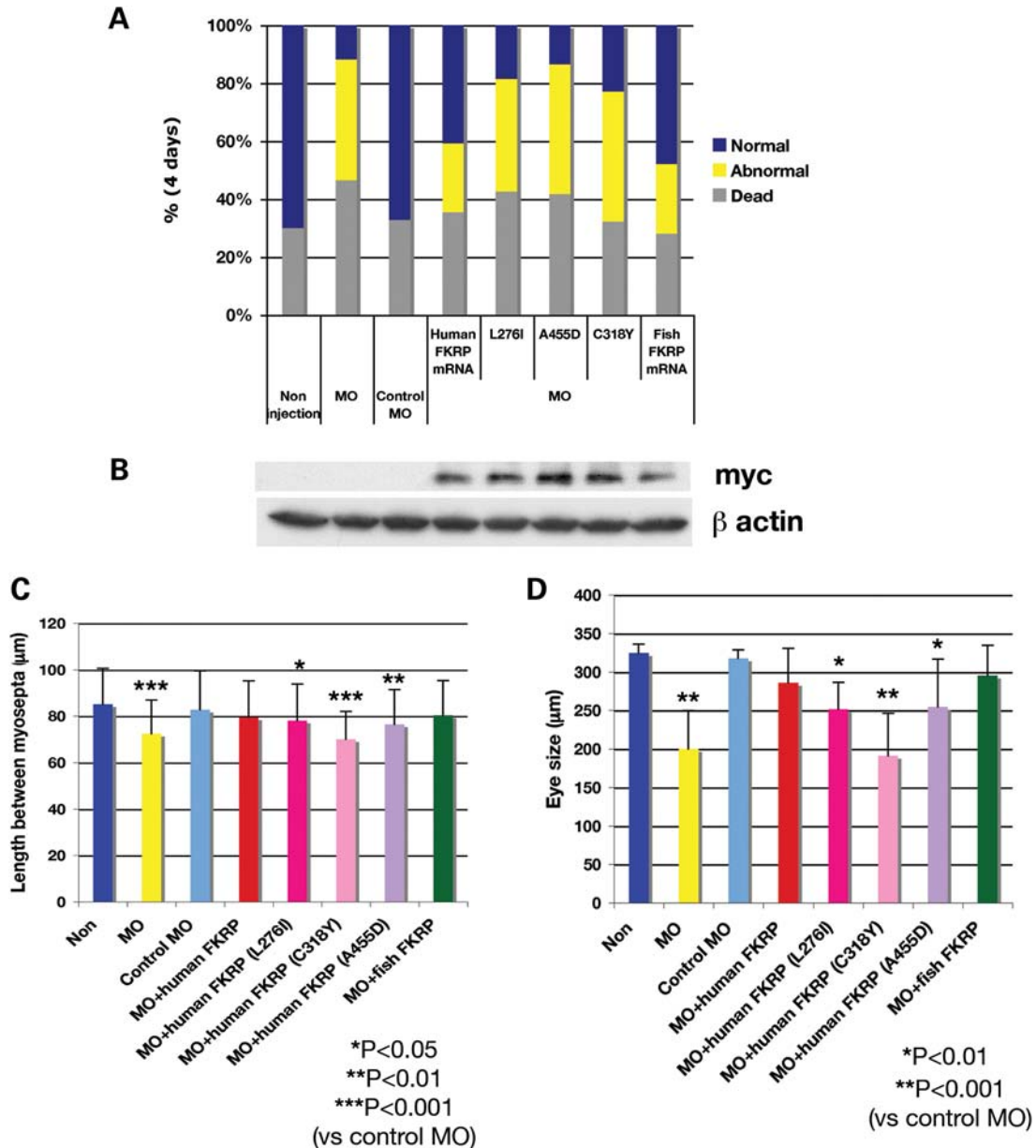
Figure 4. Restoration of normal development of FKRP morphant with co-injection of human and fish FKRP mRNA. (**A**) Histogram of the percentage of dead, affected fish of morphants and recovered fish. Blue bar shows normal %, yellow shows affected % and gray shows dead fish %. (**B**) Immunoblot analysis of 4 dpf fish extract with anti c-myc for detection of transcripts from the injected mRNA. β-Actin is used as the internal control. (**C**) Analysis of the length between myosepta. Error bars represent standard divisions. Single asterisk indicates Student's *t*-test $P < 0.05$. Double asterisks indicate $P < 0.01$. Triple asterisks indicate $P < 0.001$. (**D**) Analysis of the diameter of eye. Single asterisk indicates Student's *t*-test $P < 0.01$ and double asterisks indicate $P < 0.001$.

mRNA mutant allele injected fish. L276I-mutated fish showed an intermediate phenotype comparing the length between myosepta (78.2 μm versus control 82.8 μm) and eye diameter (252 μm versus control 324 μm). However, injection of the C318Y- and A455D-mutated mRNAs yielded a similar result to fish completely knocked down for the expression of FKRP (Fig. 4A). The eye diameter and the length between myosepta, for C318Y mutant, was smaller compared with the L276I- and A455D-mutated fish (C318Y mutant: the length between myosepta = 70 μm and eye diameter = 191 μm; A455D mutant: the length between myosepta = 76.4 μm and eye diameter = 255 μm) (Fig. 4C and D).

Recovery of muscle organization and glycosylation of α-dystroglycan

When normal human and/or fish FKRP mRNA was co-injected, birefringence of the fish was restored to normal compared with morphants alone and mutated FKRP human mRNAs (Fig. 5C–E). The normal mRNA co-injected fish had a regularity of myosepta similar to that found in wild-type (Fig. 5C and D). Co-injected L276I mutant mRNAs results in mutant fish having nearly normal birefringence in skeletal muscle compared with other mutant fish embryos. The fish co-injected with the C318Y mutant mRNA had decreased
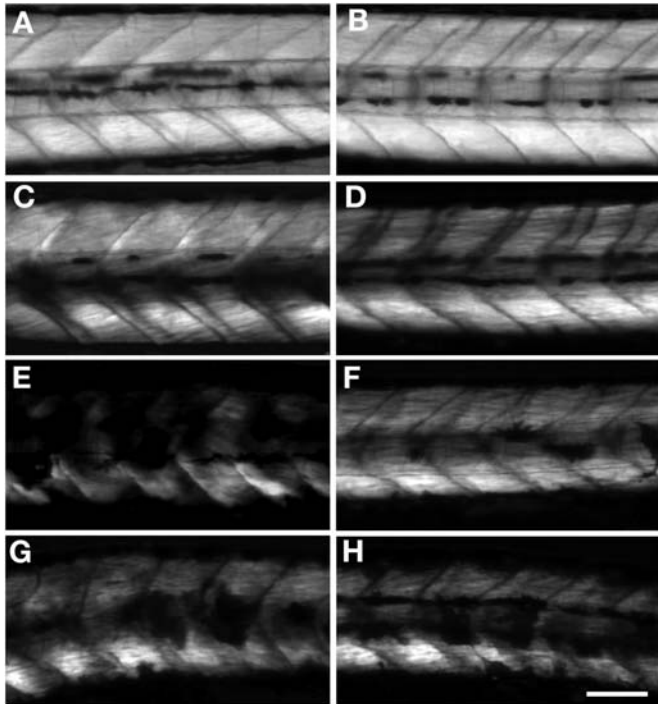
Figure 5. Birefringence assay of various FKRP injected fish at 4 days. (**A**) Wild-type fish. (**B**) Control MO2. (**C**) Normal FKRP mRNA co-injected fish. (**D**) Human normal FKRP mRNA co-injected fish. (**E**) FKRP MO2 injected fish. (**F**) Human mutated FKRP mRNA (L276I) co-injected fish. (**G**) Human mutated FKRP mRNA (C318Y) co-injected fish. (**H**) Human mutated FKRP mRNA (A455D) co-injected fish. Bar: 100 μm.

signal and no regularity of myosepta (Fig. 5G). A455D mutant mRNA showed no recovery of normal birefringence (Fig. 5H). When normal human FKRP mRNA was co-injected, the glycosylation of α-dystroglycan was restored (Fig. 6C). Co-injection of the L276I mutant mRNA lead to the boundary at myosepta that was sharp compared with other mutants (Fig. 6D). The other two mutant alleles, C318Y and A455D, had weaker glycosylation signals compared with L276I mutant and control fish and very similar to that seen with the morpholino alone.

To investigate the laminin-binding ability of α-dystroglycan from FKRP morphant embryos, we examined morphants co-injected control FKRP mRNA and mutated FKRP mRNA, and measured α-dystroglycan-binding ability using the laminin overlay assay and immunoblot with anti α-dystroglycan.

The binding of laminin to α-dystroglycan purified from 4 dpf fish tissue was found to be at a lower molecular weight compared with those from mouse muscle tissue and adult tissues (Fig. 6G, lane 1 and 2). The band was also detected with anti-α-dystroglycan (VIA4-1). Alpha-dystroglycan had a lower molecular weight compared with those of adult fish that were previously observed in laminin overlay binding (34). The laminin-binding of α-dystroglycan from FKRP morphant embryos was found to be significantly reduced compared with control and control FKRP mRNA injected FKRP morphant (Fig. 6G, lane 3 and 4). Alpha-dystroglycan purified from FKRP morphants co-injected with control FKRP mRNAs showed that the affinity to

α-dystroglycan was recovered compared with FKRP morphants (Fig. 6G, lane 5).

The binding ability of α-dystroglycan from FKRP morphant co-injected L276I mutated FKRP RNA was found to be similar to the control (Fig. 6G, lane 6); however, FKRP morphants co-injected mutated FKRP (C318Y or A455D) showed reduced binding ability compared with control (Fig. 6G, lane 7 and 8).

In FKRP morphant embryos, the distance between the myosepta was reduced and the gap between myofibers was greater. To examine the nature of the protein structure at the gap, myofibers in mutant fish were examined by immunostaining with anti-MHC and anti-laminin. In control and human normal FKRP mRNA co-injected fish, the myofibers were adjacent at myosepta (Fig. 7A and B). The gaps between myofibers that were found in FKRP morphants (Fig. 7C) were also reduced with the injection of normal human FKRP mRNA (Fig. 7B). The length of myofibers was of similar size to that seen in control (Fig. 7A). Using the L276I mutant allele, the gap was reduced compared with FKRP morphants alone and the other two mutant alleles, C318Y and A455D (Fig. 7D). In C318Y and A455D mutant alleles, the gap was still wide and myofibers were disturbed (Fig. 7E and F) similar to that seen with the FKRP morphant alone.

DISCUSSION

Knockdown of FKRP levels by morpholinos during zebrafish development results in a clear disorganization of their skeletal muscle. Abnormalities were not only confined to skeletal muscle but also in neurological tissues including the eye and there were clear heart abnormalities. It is known that mutations in the FKRP gene are associated with a spectrum of neuromuscular human diseases ranging from very mild LGMD2I to severe MDC1C and the most severe types called MEB and WWS with neurological and ocular abnormalities (13,18,36). Similar to what is observed in patients with human mutations, FKRP morphant embryos had reduction in eye diameter and muscle abnormalities, similar to results seen by others (34). These results suggest that FKRP morphants have characteristics which parallel clinical findings in human patients. In LGMD2I and MDC1C patients, clinical findings in muscle and dilated cardiomyopathy have been reported (37–40). The findings in these FKRP morphants suggest that FKRP morphant fish may have the characteristics similar to myopathy, neuropathy and cardiomyopathy system involvement in human disease. Using this fish model, further studies focused on brain, eyes and heart may be useful for understanding the mechanism of diseases in these systems.

In skeletal muscle, FKRP morphant fish have disturbed glycosylation of α-dystroglycan and abnormal muscle structure including myofiber size and an apparent gap at the myosepta. Previous reports have also showed the effects on the glycosylation of α-dystroglycan and on binding to the ECM ligand laminin (34). The linking between α-dystroglycan and ECM proteins with sugar chain of α-dystroglycan is known to be important for supporting stable muscle structures. These structures rely on the effective glycosylation of α-dystroglycan and carbohydrate modifications and are either absent or reduced
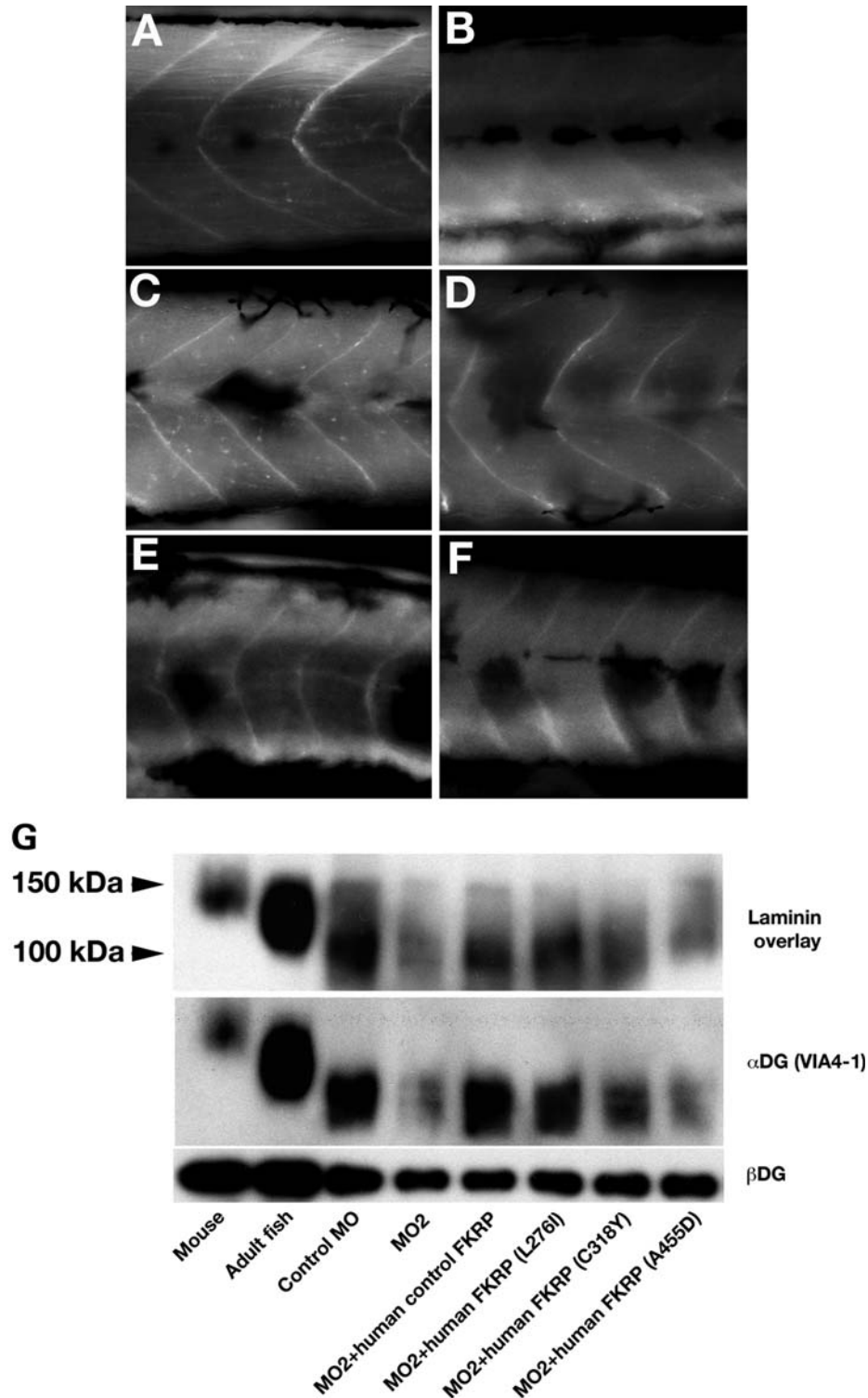
Figure 6. Glycosylation abnormalities of α-dystroglycan and recovery of glycosylation by co-injection of FKRP mRNA with MO2. (**A**–**F**) Immunostaining of 4 dpf fish co-injected FKRP mRNA with anti α-dystroglycan (VIA4-1). (A) Control MO2. (B) FKRP MO2 injected fish. (C) Human normal FKRP mRNA co-injected fish. (D) Human mutated FKRP mRNA (L276I) co-injected fish. (E) Human mutated FKRP mRNA (C318Y) co-injected fish. (F) Human mutated FKRP mRNA (A455D) co-injected fish. Bar: 100 μm. (**G**) laminin overlay assay and western blot with α- and β-dystroglycan antibody.

resulting in a predicted decrease in binding of α-dystroglycan to its ligands (41). A muscle degenerative phenotype has also been described in morpholino-directed dystroglycan knockdown fish embryos in which there is a disruption of the DGC resulting in abnormalities in muscle fiber organization (42).
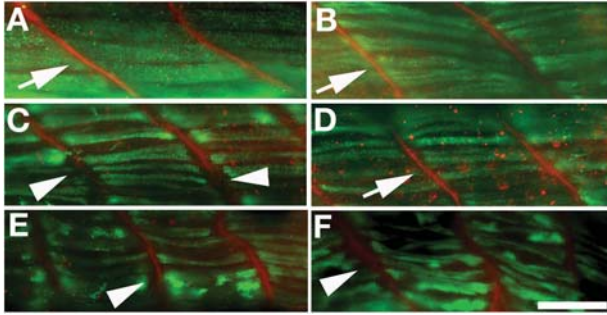
Figure 7. The gaps between myofibers can be repaired by co-injection of normal FKRP mRNA with MO2 but not all human mutant alleles. Co-immunostaining of 4 dpf fish co-injected FKRP mRNA with anti MHC (green) and anti laminin (red). (**A**) Control MO2. (**B**) Human normal FKRP mRNA co-injected fish. (**C**) FKRP MO2 injected fish. (**D**) Human mutated FKRP mRNA (L276I) co-injected fish. (**E**) Human mutated FKRP mRNA (C318Y) co-injected fish. (**F**) Human mutated FKRP mRNA (A455D) co-injected fish. Bar: 50 μm. In control and human control mRNA co-injected fish, the myofibers are adjacent at myosepta (arrows in A and B); however, FKRP morphant has the gap between myosepta (arrowhead in C). In L276I mutant fish, the gap is also narrowed (arrow in D). In C318Y and A455D mutant fish, there still remain gaps similar to that found in FKRP morphant fish (arrows in E and F).

The expression of dystrophin and β-dystroglycan was normal in the skeletal muscle of FKRP morphant; however, myosepta were irregular and there is a wide gap between myofibers when compared with the control. These findings indicate that modification of sugar chains on α-dystroglycan may play a critical role in maintaining myosepta length and the spacing between myosepta. The lack of sugar modification likely causes a disconnection between myofibers, and the muscle degeneration decreased upon birefringence.

Somewhat surprising was the observation that the human FKRP protein functions to partially restore normal fish muscle structure. In addition, human FKRP mRNA with mutations causing muscular dystrophy in humans is less effective at restoring structure compared with normal human FKRP. This suggests that FKRP functions in the glycosylation of α-dystroglycan thus making this model particularly appropriate for studies on the group of human diseases caused by FKRP mutations. This model could also be used to map domains on the human and fish FKRP proteins which are important for normal development and function.

Interestingly, the FKRP morphants co-injected with human FKRP mutations have a wide phenotypic range. In the LGMD2I model fish with L276I mutation, the phenotypes were generally mild similar to human patients with this mutation. In LGMD2I patient, the clinical findings in muscle and heart are mild compared with CMD (18). The reduced abnormalities and laminin binding ability of α-dystroglycan in fish co-injected with the human L276I mutation are consistent with human relatively mild clinical finding course.

The zebrafish models exhibited phenotypes similar to the severe CMD and WWS with C318Y and MDC1C with A455D mutations. In MDC1C, the muscle clinical findings are severe (13) and in WWS, the clinical findings include neurological, heart and skeletal muscle (22) and analogous to this. C318Y mutation had abnormalities in eye formation similar to those seen in WWS human patients.

In conclusion, these fish models of the human disease may be very useful for understanding the pathogenesis of diseases caused by mutations in the FKRP gene. Further investigation using these knockdown fish models and those fish bearing human mutations which yield similar phenotypes to human disease may give clues to the function of FKRP in the glycosylation of α-dystroglycan and the maintaining of normal muscle. These studies aid our understanding of the phenotypic spectrum in human muscular dystrophies associated with mutations in the FKRP gene and these fish models are very useful in testing for therapeutic compounds for these muscular dystrophies.

MATERIALS AND METHODS

Fish strains and maintenance

The zebrafish wild-type strain (AB) was used in this study. Zebrafish embryos were collected and raised at 28.5°C according to standard procedures (43) and staged in hours or days post-fertilization (hpf or dpf) according to standard criteria (44).

Anti-sense MO injection

Anti-sense MO (Gene Tools LLC) targeted to interfere with FKRP translation were designed using the 5′ sequence around the putative start of translation of the zebrafish FKRP mRNA (NCBI accession number NM_001042689). The morpholino sequences were FKRP MO 1: 5′-TGGCAAAAACTGATAC GCATTATGG-3′, FKRP MO 2: 5′-CTTGTGGTTTTATGGC AGAAAGAGT-3′. For control MO, we used two 5 mis-sequence control morpholino, mis-Control MO1: 5′-TGcC AtAAACTcATACcCATTATGc-3′, mis-Control MO2: 5′-CTTcTGcTTTTATGcCAcAAAcAGT-3′ (five mismatched nucleotides in lower case). Morpholinos were re-suspended in 1x Danieau solution [58 mM NaCl, 0.7 mM KCl, 0.4 mM MgSO$_4$, 0.6 mM Ca (NO$_3$)$_2$, 5 mM HEPES; pH 7.6] with 0.1% phenol red as an injection indicator. Morpholinos were injected into the yolk of one-cell- to two-cell-stage embryos. Embryos were injected with 1.5–12 ng of morpholino depending on experimental condition.

Cloning of zebrafish and human FKRP

Zebrafish total RNA was extracted from 1 dpf wild-type embryos and purified with RNeasy micro kit (QIAGEN) and total RNA (500 ng) was converted to cDNA using SuperScript III first-strand system for RT–PCR (Invitrogen) according to the manufacturer's protocol. Primers used to amplify the full-length fish FKRP cDNA coding sequence were forward: 5′-CCATAATGCGTATCAGTTTTTTGCCAGG-3′, reverse: 5′-TTCCCAAACAATGCACACAC-3′. The PCR product of the full-length FKRP cDNA was cloned into pGEM easy-T-vector (Stratagene). The FKRP gene sequence was confirmed by sequence analysis and the cDNA then cloned into pcDNA3.1/myc-His C (Invitrogen). PCR products of C-terminal region that amplified sequences with forward primer: 5′-ATGTTTCGGGACAGTTCGAG-3′, reverse primer: 5′-CG AGCGGCCGCCGATCCAAATGTGCG-3′, were inserted into

the fish FKRP cDNA construct in pcDNA 3.1C after digestion with Afe I & Not I (New England Biolads).

Human FKRP full-length cDNA was amplified by PCR using a forward primer: 5′- CCAGCTAGCCCCAGACTTC-3′, reverse primer: 5′-CTTGGTCAGTTTCCCCCTTC-3′ using human normal skeletal muscle cDNA (Invitrogen) as a template. The PCR product of the full-length human FKRP cDNA was cloned into pGEM easy-T-vector (Stratagene). The cDNA clones were sequenced to confirm the fidelity of FKRP sequences. The cDNA was cloned into pcDNA3.1/myc-His C. PCR product of C-terminal sequence amplified by PCR with forward primer: 5′-ACGCCCGCCTACCTC TAC-3′, reverse primer: 5′-GGTGACCTCGAGCGCCGC TTCCCGTCAGACTCAGC-3′. The product was ligated into FKRP cDNA in pcDNA3.1/myc-His C after digestion with Xho I (New England Biolads).

All PCR products and cloned fragments were sequenced by the Molecular Genetics Core Facility at Children's Hospital Boston using sequencing primers for FKRP sequence analysis (Supplement Data S3).

Generation of expression constructs and *in vitro* transcription of RNAs

Both human and fish FKRP, full-length FKRP mRNAs with myc and His tag constructs were cloned into the pCS2+ expression vector. With human FKRP constructs, two different amino acid substitutions, the same as mutations found MDC1C (1364C > A, A455D) and LGMD2I (826C > A, L276I) patients, were incorporated into the expression vector by site-directed mutagenesis kit (Stratagene). Primers for mutagenesis were forward primer: 5′-GGTGCCCCTGCCC TTTGACGGCTTCGTGG-3′, reverse primer: 5′-CCACGAA GCCGTCAAAGGGCAGGGGCACC-3′: for the MDC1C causative mutation (1364C > A, A455D). The forward primer: 5′-GGCATCCGCATAGTGAGCTGGGAAGGC-3′, reverse primer: 5′-GCCTTCCCAGCTCACTAGGCGGAT GCC-3′: were used for the LGMD2I causative mutation (826C > A, L276I). For insertion of WWS causative mutation (953G > A, C318Y), the PCR product that amplified by forward primer: 5′-AGCGCTGGACGCCCCCCTGCTACCT GCGCGCGCTGCGCG-3′, reverse primer: 5′-GGTCCACGT CGTAGTCCCATGG-3′ was inserted to human FKRP cDNA construct in pCS2+ after digestion with *Afe*I and *Nco*I. All clones were sequenced to confirm that only the intended mutations were incorporated into the constructs. RNAs were synthesized from Asp718-digested pCS2+ plasmids using the *sp6* mMessage mMachine kit (Ambion). The RNAs were quantified by nano drop (Thermo scientific). Phenol red (0.1%) was added to the RNA solution as a tracer, and mRNAs (100 pg) were co-injected into 1-cell-stage embryos with FKRP MO2. Following injection, embryos were cultured in aquatic system at 28.5°C.

Birefringence

Muscle birefringence was analyzed as previously described (45) by placing anesthetized embryos on a glass polarizing filter and covering the embryos with second polarizing filter. The filters were then placed on an underlit dissecting scope (Nicon, model SMZ1500) and the top polarizing filter twisted until only the light refracting through the striated muscle was visible. Since the degree of birefringence is affected by the horizontal orientation of the fish, the fish were gently oscillated back and forth to account for differences in positioning.

Zebrafish FKRP antibody

An antibody directed against zebrafish FKRP was produced by Invitrogen custom service with synthesized peptides (C + NPQYPNPAKKRLDRSR; 517-530) as an antigen. The synthesized peptides were used to absorb the antibodies as a control for specificity of this antibody.

Immunohistochemistry

For immunohistochemical staining of whole fish, embryos were stored in 100% methanol at −20°C after fixation with 4% PFA overnight at 4°C. Following rehydration with methanol series (70–50% and PBS-T) and blocking with 2% casein, 1% BSA, 0.05% Tween 20 in PBS to reduce non-specific binding, embryos were incubated separately with the following antibodies: anti-dystrophin (1:100, Sigma), anti β-dystroglycan (1:100, Novocastra), anti α-dystroglycan (1:50, VIA4-1, Millipore), anti-MHC (1:50, F59, Hybridoma bank) and anti-laminin (1:100, Sigma) at 4°C overnight. After washing several times, the samples were incubated with secondary antibodies (1:500, either anti-mouse AlexaFluor-488 or anti-rabbit AlexaFluor-568, Invitrogen). The stained embryos were observed under the dissection scope (Nikon, SMZ1500) with EXFO Fluorescence illumination system, X-Cite 120 (Photonic Solution Inc.), a Nikon Eclipse E-1000 microscope, photographed using a Hamamatsu digital camera, and images were acquired using Openlab software version 3.1.5 (Improvision).

Measurement of eye diameter and distance between myosepta

The diameter of the eye of 4 dpf embryos was measured under a dissection scope (Nicon, SMZ1500) with Open lab software (Improvision). The distance between myosepta was measured with Open lab software (Improvision) under the dissection scope (Nikon, SMZ1500) after immunostaining of 4 dpf embryos with anti-β-dystroglycan. Measurements started near the head for 10 subsequent myosepta.

Western blotting

Dechorinated and deyolked embryos were homogenized in Tris-buffered saline (TBS) containing 2% Triton X-100 and protease inhibitors. Following centrifugation at 14000*g* at 4°C for 20 min, the concentration of protein in supernatants was determined by Bradford method, using a protein assay kit (Bio-rad). Proteins were separated by electrophoresis on 8–16% gradient Tris-glycine gels (Invitrogen) and transferred onto PVDF membrane (Invitrogen). After blocking the membrane in PBS containing 1% BSA, 2% casein, blotted proteins were incubated with primary antibody, anti fish FKRP (1:100),

anti c-myc (1:100, BD bioscience) anti β-actin (1:500, Sigma). After washing, the membranes were incubated with horse-radish peroxidase secondary antibody (anti-rabbit or mouse IgG, 1:15000, Invitrogen). Proteins were detected using a western blotting detection kit (Millipore).

Laminin overlay assay

Laminin overlay assays were performed using mouse Engelbreth-Holm-Swarm (EHS) laminin (Sigma) as previous described (17). For the purification of a dystroglycan, wheat germ agglutinin (WGA)-agarose beads (Vector Labs) were added to extracts containing equal amounts of total protein and incubated overnight at 4°C followed by elution from WGA beads with SDS sample buffer. Tissue extracts were made from adult zebrafish (4-month-old fish) and adult mouse muscle. Proteins were separated by electrophoresis on 4–12% gradient Tris-glycine gels (Invitrogen) and transferred onto PVDF membrane (Invitrogen). PVDF membranes blotted proteins were blocked in the binding buffer (10 mM triethanolamine, 140 mM NaCl, 1 mM $MgCl_2$, 1 mM $CaCl_2$, pH 7.6) containing 5% non-fat dry milk followed by incubation with laminin overnight. Membranes were incubated with rabbit anti-laminin (1:5000, Sigma) followed by anti-rabbit IgG-HRP (1:15000, Invitrogen). Proteins were detected using a western blotting detection kit (Millipore). For detection of α- and β-dystroglycan, anti-α-dystroglycan (1:50, VIA4-1, Millipore) and anti-β-dystroglycan (1:100, Novocastra) were used.

SUPPLEMENTARY MATERIAL

Supplementary Material is available at *HMG* online.

REFERENCES

1. Williamson, R.A., Henry, M.D., Daniels, K.J., Hrstka, R.F., Lee, J.C., Sunada, Y., Ibraghimov-Beskrovnaya, O. and Campbell, K.P. (1997) DG is essential for early embryonic development: disruption of Reichert's membrane in Dag1-null mice. *Hum. Mol. Genet.*, **6**, 831–841.
2. Ibraghimov-Beskrovnaya, O., Ervasti, J.M., Leveille, C.J., Slaughter, C.A., Sernett, S.W. and Campbell, K.P. (1992) Primary structure of dystrophin-associated glycoproteins linking dystrophin to the extracellular matrix. *Nature*, **355**, 696–702.
3. Ervasti, J.M. and Campbell, K.P. (1993) A role for dystrophin-associated glycoprotein complex as a transmembrane linker between laminin and actin. *J. Cell Biol.*, **122**, 809–823.
4. Campanelli, J., Roberds, S., Campbell, K. and Scheller, R. (1994) A role for dystrophin-associated glycoproteins and utrophin in agrin-induced AchR clustering. *Cell*, **77**, 663–674.
5. Sugita, S., Saito, F., Tang, J., Satz, J., Campbell, K. and Sudhof, T.C. (2001) A stoichiometric complex of neurexins and dystroglycan in brain. *J. Cell Biol.*, **154**, 435–445.
6. Cohn, R.D. (2005) DG: important player in skeletal muscle and beyond. *Neuromuscul. Disord.*, **15**, 207–217.
7. van Reeuwijk, J., Brunner, H.G. and van Bokhoven, H. (2005) Glyc-O-genetics of Walker–Warburg syndrome. *Clin. Genet.*, **67**, 281–289.
8. Yoshida, A., Kobayashi, K., Manya, H., Taniguchi, K., Kano, H., Mizuno, M., Inazu, T., Mitsuhashi, H., Takahashi, S., Takeuchi, M. *et al.* (2001) Muscular dystrophy and neuronal migration disorder caused by mutations in a glycosyltransferase, POMGnT1. *Dev. Cell*, **1**, 717–724.
9. Beltrán-Valero de Bernabé, D., Currier, S., Steinbrecher, A., Celli, J., van Beusekom, E., van der Zwaag, B., Kayserili, H., Merlini, L., Chitayat, D., Dobyns, W.B. *et al.* (2002) Mutations in the O-mannosyltransferase gene POMT1 give rise to the severe neuronal migration disorder Walker–Warburg syndrome. *Am. J. Hum. Genet.*, **71**, 1033–1043.
10. van Reeuwijk, J., Janssen, M., van den Elzen, C., Beltran-Valero de Bernabé, D., Sabatelli, P., Merlini, L., Boon, M., Scheffer, H., Brockington, M., Muntoni, F. *et al.* (2005) POMT2 mutations cause alpha-dystroglycan hypoglycosylation and Walker–Warburg syndrome. *J. Med. Genet.*, **12**, 907–912.
11. Kobayashi, K., Nakahori, Y., Miyake, M., Matsumura, K., Kondo-Iida, E., Nomura, Y., Segawa, M., Yoshioka, M., Saito, K., Osawa, M. *et al.* (1998) An ancient retrotransposal insertion causes Fukuyama-type congenital muscular dystrophy. *Nature*, **394**, 388–392.
12. Grewal, P.K., Holzfeind, P.J., Bittner, R.E. and Hewitt, J.E. (2001) Mutant glycosyltransferase and altered glycosylation of alpha-DG in the myodystrophy mouse. *Nat. Genet.*, **28**, 151–154.
13. Brockington, M., Blake, D.J., Prandini, P., Brown, S.C., Torelli, S., Benson, M.A., Ponting, C.P., Estournet, B., Romero, N.B., Mercuri, E. *et al.* (2001a) Mutations in the fukutin-related protein gene (FKRP) cause a form of congenital muscular dystrophy with secondary laminin alpha2 deficiency and abnormal glycosylation of alpha-DG. *Am. J. Hum. Genet.*, **69**, 1198–1209.
14. Holzfeind, P.J., Grewal, P.K., Reitsamer, H.A., Kechvar, J., Lassmann, H., Hoeger, H., Hewitt, J.E. and Bittner, R.E. (2002) Skeletal, cardiac and tongue muscle pathology, defective retinal transmission, and neuronal migration defects in the Large (myd) mouse defines a natural model for glycosylation-deficient muscle–eye–brain disorders. *Hum. Mol. Genet.*, **11**, 2673–2687.
15. Willer, T., Prados, B., Falcón-Pérez, J.M., Renner-Müller, I., Przemeck, G.K., Lommel, M., Coloma, A., Valero, M.C., de Angelis, M.H., Tanner, W. *et al.* (2004) Targeted disruption of the Walker–Warburg syndrome gene Pomt1 in mouse results in embryonic lethality. *Proc. Natl Acad. Sci. USA*, **101**, 14126–14131.
16. Straub, V. and Bushby, K. (2006) The childhood limb-girdle muscular dystrophies. *Semin. Pediatr. Neurol.*, **13**, 104–114.
17. Michele, D.E., Barresi, R., Kanagawa, M., Saito, F., Cohn, R.D., Satz, J.S., Dollar, J., Nishino, I., Kelley, R.I., Somer, H. *et al.* (2002)

Post-translational disruption of DG-ligand interactions in congenital muscular dystrophies. *Nature*, **418**, 417–422.

18. Brockington, M., Yuva, Y., Prandini, P., Brown, S.C., Torelli, S., Benson, M.A., Herrmann, R., Anderson, L.V., Bashir, R., Burgunder, J.M. *et al.* (2001b) Mutations in the fukutin-related protein gene (FKRP) identify limb girdle muscular dystrophy 2I as a milder allelic variant of congenital muscular dystrophy MDC1C. *Hum. Mol. Genet.*, **10**, 2851–2859.

19. Aravind, L. and Koonin, E.V. (1999) The fukutin protein family-predicted enzymes modifying cell-surface molecules. *Curr. Biol.*, **9**, R836–R837.

20. Sveen, M.L., Schwartz, M. and Vissing, J. (2006) High prevalence and phenotype-genotype correlations of limb girdle muscular dystrophy type 2I in Denmark. *Ann. Neurol.*, **59**, 808–815.

21. Louhichi, N., Triki, C., Quijano-Roy, S., Richard, P., Makri, S., Méziou, M., Estournet, B., Mrad, S., Romero, N.B., Ayadi, H. *et al.* (2004) New FKRP mutations causing congenital muscular dystrophy associated with mental retardation and central nervous system abnormalities. Identification of a founder mutation in Tunisian families. *Neurogenetics*, **5**, 27–34.

22. Beltran-Valero de Bernabé, D., Voit, T., Longman, C., Steinbrecher, A., Straub, V., Yuva, Y., Herrmann, R., Sperner, J., Korenke, C., Diesen, C. *et al.* (2004) Mutations in the FKRP gene can cause muscle–eye–brain disease and Walker–Worburg syndrome. *J. Med. Genet.*, **41**, 61–65.

23. Mercuri, E., Topaloglu, H., Brockington, M., Berardinelli, A., Pichiecchio, A., Santorelli, F., Rutherford, M., Talim, B., Ricci, E., Voit, T. *et al.* (2006) Spectrum of brain changes in patients with congenital muscular dystrophy and FKRP gene mutations. *Arch. Neurol.*, **63**, 251–257.

24. Bassett, D.I., Bryson-Richardson, R.J., Daggett, D.F., Gautier, P., Keenan, D.G. and Currie, P.D. (2003) Dystrophin is required for the formation of stable muscle attachments in the zebrafish embryo. *Development*, **130**, 5851–5860.

25. Bassett, D.I. and Currie, P.D. (2003) The zebrafish as a model for muscular dystrophy and congenital myopathy. *Hum. Mol. Genet.*, **12**, 265–270.

26. Kunkel, L.M., Bachrach, E., Bennett, R.R., Guyon, J. and Steffen, L. (2006) Diagnosis and cell-based therapy for Duchenne muscular dystrophy in humans, mice, and zebrafish. *J. Hum. Genet.*, **51**, 397–406.

27. Guyon, J.R., Mosley, A.N., Jun, S.J., Montanaro, F., Steffen, L.S., Zhou, Y., Nigro, V., Zon, L.I. and Kunkel, L.M. (2005) Delta-sarcoglycan is required for early zebrafish muscle organization. *Exp. Cell. Res.*, **304**, 105–115.

28. Guyon, J.R., Mosley, A.N., Zhou, Y., O'Brien, K.F., Sheng, X., Chiang, K., Davidson, A.J., Volinski, J.M., Zon, L.I. and Kunkel, L.M. (2003) The dystrophin associated protein complex in zebrafish. *Hum. Mol. Genet.*, **12**, 601–615.

29. Guyon, J.R., Steffen, L.S., Howell, M.H., Pusack, T.J., Lawrence, C. and Kunkel, L.M. (2007) Modeling human muscle disease in zebrafish. *Biochim. Biophys. Acta*, **1772**, 205–215.

30. Hall, T.E., Bryson-Richardson, R.J., Berger, S., Jacoby, A.S., Cole, N.J., Hollway, G.E., Berger, J. and Currie, P.D. (2007) The zebrafish candyfloss mutant implicates extracellular matrix adhesion failure in laminin

31. Guyon, J.R., Goswami, J., Jun, S.J., Thorne, M., Howell, M., Pusack, T., Kawahara, G., Steffen, L.S., Galdzicki, M. and Kunkel, L.M. (2009) Genetic isolation and characterization of a splicing mutant of zebrafish dystrophin. *Hum. Mol. Genet.*, **18**, 202–211.

32. Steffen, L.S., Guyon, J.R., Vogel, E.D., Beltre, R., Pusack, T.J., Zhou, Y., Zon, L.I. and Kunkel, L.M. (2007) Zebrafish orthologs of human muscular dystrophy genes. *BMC Genomics*, **8**, 79.

33. Moore, C.J., Goh, H.T. and Hewitt, J.E. (2008) Genes required for functional glycosylation of dystroglycan are conserved in zebrafish. *Genomics*, **92**, 159–167.

34. Thornhill, P., Bassett, D., Lochmüller, H., Bushby, K. and Straub, V. (2008) Developmental defects in a zebrafish model for muscular dystrophies associated with the loss of fukutin-related protein (FKRP). *Brain*, **131**, 1551–1561.

35. Ervasti, J.M. and Campbell, K.P. (1993) A role for the dystrophin-glycoprotein complex as a transmembrane linker between laminin and actin. *J. Cell Biol.*, **122**, 809–823.

36. Mercuri, E., Brockington, M., Straub, V., Quijano-Roy, S., Yuva, Y., Herrmann, R., Brown, S.C., Torelli, S., Dubowitz, V., Blake, D.J. *et al.* (2003) Phenotypic spectrum associated with mutations in the fukutin-related protein gene. *Ann. Neurol.*, **53**, 537–542.

37. Poppe, M., Cree, L., Bourke, J., Eagle, M., Anderson, L.V., Birchall, D., Brockington, M., Buddles, M., Busby, M., Muntoni, F. *et al.* (2003) The phenotype of limb-girdle muscular dystrophy type 2I. *Neurology*, **60**, 1246–1251.

38. Poppe, M., Bourke, J., Eagle, M., Frosk, P., Wrogemann, K., Greenberg, C., Muntoni, F., Voit, T., Straub, V., Hilton-Jones, D. *et al.* (2004) Cardiac and respiratory failure in limb-girdle muscular dystrophy 2I. *Ann. Neurol.*, **56**, 738–741.

39. Muller, T., Krasnianski, M., Witthaut, R., Deschauer, M. and Zierz, S. (2005) Dilated cardiomyopathy may be an early sign of the C826A Fukutin-related protein mutation. *Neuromuscl. Disord.*, **15**, 372–376.

40. Gaul, C., Deschauer, M., Tempelmann, C., Vielhaber, S., Klein, H.U., Heinze, H.J., Zierz, S. and Grothues, F. (2006) Cardiac involvement in limb-girdle muscular dystrophy 2I: conventional cardiac diagnostic and cardiovascular magnetic resonance. *J. Neurol.*, **253**, 1317–1322.

41. Barresi, R. and Campbell, K.P. (2006) DG: from biosynthesis to pathogenesis of human disease. *J. Cell. Sci.*, **119**, 199–207.

42. Parsons, M.J., Campos, I., Hirst, E.M.A. and Stemple, D.L. (2002a) Removal of DG causes severe muscular dystrophy in zebrafish embryos. *Development*, **129**, 3505–3512.

43. Nusslein-Volhard, C. and Dahm, R. (2002) *Zebrafish: A Practical Approach*, Oxford University press.

44. Kimmel, C.B., Ballard, W.W., Kimmel, S.R., Ullmann, B. and Schilling, T.F. (1995) Stages of embryonic development of the zebrafish. *Dev. Dyn.*, **203**, 253–310.

45. Granato, M., van Eeden, F.J., Schach, U., Trowe, T., Brand, M., Furutani-Seiki, M., Haffter, P., Hammerschmidt, M., Heisenberg, C.P., Jiang, Y.J. *et al.* (1996) Genes controlling and mediating locomotion behavior of the zebrafish embryo and larva. *Development*, **123**, 399–413.